Mon. Not. R. Astron. Soc. **368,** 1500–1506 (2006) doi:10.1111/j.1365-2966.2006.10244.x

Magnetic fields in the centre of the Perseus cluster

G. B. Taylor,[1,2⋆] N. E. Gugliucci,[2,3⋆] A. C. Fabian,[4⋆] J. S. Sanders,[4⋆] G. Gentile[1⋆] and S. W. Allen[5⋆]

[1]*Department of Physics and Astronomy, University of New Mexico, Albuquerque, NM 87131, USA*
[2]*National Radio Astronomy Observatory, Socorro, NM 87801, USA*
[3]*Department of Astronomy, University of Virginia, Charlottesville, VA 22903, USA*
[4]*Institute of Astronomy, Madingley Road, Cambridge CB3 0HA*
[5]*Kavli Institute of Particle Astrophysics and Cosmology, Stanford University, Stanford, CA 94305, USA*

Accepted 2006 February 23. Received 2006 February 15; in original form 2006 January 12

ABSTRACT

We present Very Long Baseline Array (VLBA) observations of the nucleus of NGC 1275, the central, dominant galaxy in the Perseus cluster of galaxies. These are the first observations to resolve the linearly polarized emission from 3C 84, and from them we determine a Faraday rotation measure (RM) ranging from 6500 to 7500 rad m^{-2} across the tip of the bright southern jet component. At 22 GHz some polarization is also detected from the central pc of 3C 84, indicating the presence of even more extreme RMs that depolarize the core at lower frequencies. The nature of the Faraday screen is most consistent with being produced by magnetic fields associated with the optical filaments of ionized gas in the Perseus cluster.

Key words: accretion, accretion discs – galaxies: clusters: individual: Perseus – intergalactic medium – radio continuum: galaxies.

1 INTRODUCTION

The Perseus cluster, A426, is the most X-ray luminous cluster in the nearby universe, and the prototypical 'cooling core' cluster. In these cooling core clusters the radiative cooling time of the X-ray emitting gas is considerably shorter than the age of the universe, so to maintain equilibrium the gas must flow into the centre of the cluster, or another source of energy is required to reheat the gas. Since massive flows of material are not observed, the emerging solution to the energy deficit is the active galaxy that is almost always (Burns 1990) present at the centre of massive clusters. Shocks and ripples are clearly evident in the deep *Chandra* image of Perseus (Fabian et al. 2005a, 2006), and could provide steady heating of the centre of the cluster (Fabian et al. 2005b). In Perseus the active galactic nucleus (AGN) manifests itself directly as a bright radio source known as Perseus A or 3C 84, associated with the galaxy NGC 1275. 3C 84 is one of the brightest compact radio sources in the sky and has been studied in some detail (Vermeulen, Readhead & Backer 1994; Taylor & Vermeulen 1996; Silver, Taylor & Vermeulen 1998; Walker et al. 2000). In particular, it is known to undergo bursts of activity (Kellermann & Pauliny-Toth 1968; Taylor & Vermeulen 1996) that could also drive the observed shocks and sound waves through the cluster.

Faraday rotation measure (RM) observations with the Very Large Array (VLA) of radio galaxies embedded in clusters of galaxies have been used to elicit information about the magnetic field strength and topology associated with the hot cluster gas (Taylor, Barton & Ge 1994; Carilli & Taylor 2002). These magnetic fields then play an important role in modifying the energy transport and dissipation in the centre of the cluster (Fabian et al. 2005b). Comparisons between the inferred cooling flow rates (in the absence of reheating) and the maximum Faraday RM indicate a correlation, and there is some evidence that magnetic fields are enhanced at the centres of clusters (Feretti et al. 1999; Vogt & Enßlin 2005). Given the high density of gas at the centre of the Perseus cluster the Faraday RMs towards 3C 84 are expected to be well over 1000 rad m^{-2} (Taylor et al. 1994). Unfortunately such high RMs, and the correspondingly large RM gradients are difficult to measure due to cancellation of the linearly polarized signal within the telescope beam (typically 0.5 arcsec for VLA observations). Another problem with obtaining polarimetric measurements of 3C 84 with the VLA is the high dynamic range imposed by the ∼20-Jy peak flux density at centimetre wavelengths and arcsec resolution. In order to overcome these limitations, we have used simultaneous multifrequency observations of 3C 84 at high angular resolution taken using the Very Long Baseline Array (VLBA).

Throughout this paper we assume $H_0 = 71\,\mathrm{km\,s^{-1}\,Mpc^{-1}}$ so that 1 arcsec = 0.35 kpc at the redshift of NGC 1275 (0.0176; Huchra, Vogeley & Geller 1999).

2 VLBA OBSERVATIONS

Observations were centred on 4.8, 8.4, 15.1 and 22.2 GHz with the VLBA on 2004 October 26 and 2004 November 11 using the

⋆E-mail: gbtaylor@unm.edu (GBT); neg9j@virginia.edu (NEG); acf@ast.cam.ac.uk (ACF); jss@ast.cam.ac.uk (JSS); ggentile@unm.edu (GG); swa@stanford.edu (SWA)

Table 1. Observational parameters.

Source	Date	Frequency (GHz)	Time (min)	Bandwidth (MHz)	Peak (mJy beam^{-1})	rms (mJy beam^{-1})
(1)	(2)	(3)	(4)	(5)	(6)	(7)
3C 84	20041026	4.6	11	16	3200	0.52
	2004 Oct 26	5.0	11	16	3560	0.96
	2004 Oct 26	8.2	10	16	7390	1.20
	2004 Oct 26	8.5	10	16	7620	1.21
	2004 Oct 26	14.9	10	16	8960	2.27
	2004 Oct 26	15.3	10	16	8910	2.25
	2004 Oct 26	22.2	10	32	5990	7.63
3C 84	20041111	4.6	13	16	3120	0.31
	2004 Nov 11	5.0	13	16	3520	0.39
	2004 Nov 11	8.2	12	16	7430	0.56
	2004 Nov 11	8.5	12	16	7600	0.36
	2004 Nov 11	14.9	13	16	8750	1.38
	2004 Nov 11	15.3	13	16	8750	1.37
	2004 Nov 11	22.2	14	32	5940	1.36

Notes – (1) J2000 source name; (2) date of observation; (3) frequency in GHz; (4) integration time in minutes; (5) bandwidth in MHz; (6) peak in the total intensity image from the average of two adjacent IFs; (7) rms noise off source from the Stokes Q image in mJy beam^{-1} measured from the matching resolution images. Noise in Stokes I, Q and U images are similar.

VLBA.[1] In both cases, 3C 84 was being used as the leakage term calibrator for observations of Compact Symmetric Objects (Gugliucci et al. 2005). Six scans of typically 2-min duration were obtained at each frequency band. Each frequency band was separated into four IFs, and these IFs were paired for the purpose of imaging the total intensity except at 22.2 GHz where all four IFs were averaged. For the purposes of determining the polarization and subsequently the RMs each IF was imaged separately in Stokes Q and U. Observational parameters are presented in Table 1.

Amplitude calibration of the data was derived from system temperatures and antenna gains. Fringe fitting was performed with the AIPS task FRING on 3C 84. The leakage, or D-term solutions were determined with the AIPS task LPCAL on 3C 84. Absolute electric vector position angle (EVPA) calibration was determined using the EVPAs of J1310+322 and BL Lac listed in the VLA Monitoring Program[2] (Taylor & Myers 2000). Note that the EVPAs were corrected for each of the four IFs separately.

3 *CHANDRA* OBSERVATIONS

We used recent deep *Chandra* observations (Fabian et al. 2006) of the Perseus cluster to model the central density profile. In Fig. 1, we show the deprojected density profile and the projected temperature profile. Within the central 0.8 kpc (2.2 arcsec) the profile is severely affected by the nucleus so that the temperatures and densities are not representative of the properties of the intracluster medium (ICM). We estimate an average central density over the inner 2 kpc to be 0.3 cm^{-3}.

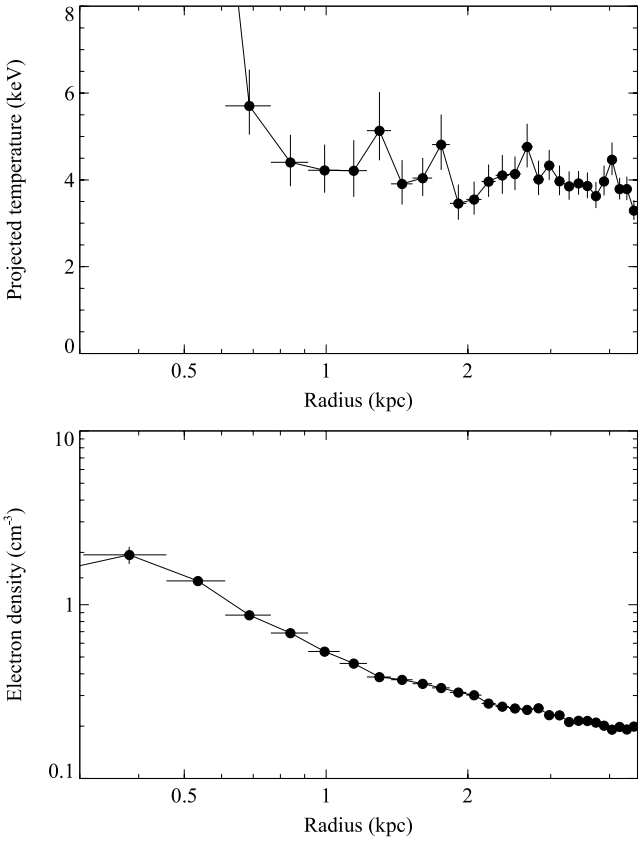

Figure 1. The temperature and density profile in the centre of the Perseus cluster derived from a long *Chandra* observation (Fabian et al. 2006).

4 RESULTS

We formed total intensity images of 3C 84 between 5 and 22 GHz. Images of similar quality are readily available in the literature (Vermeulen et al. 1994; Walker et al. 2000), so we do not reproduce them here. Instead we provide a brief summary of source properties (position, flux density, size, distance etc.) in Table 2, and we concentrate here on the polarimetry results.

[1] The National Radio Astronomy Observatory is operated by Associated Universities, Inc., under cooperative agreement with the National Science Foundation.
[2] http://www.vla.nrao.edu/astro/calib/polar/

Table 2. Source properties.

Property	3C 84
Core RA (J2000)	$03^{h}19^{m}48^{s}.1601$
Dec. (J2000)	$41^{\circ}30'42''.104$
Gal. long. (l)	150.58°
Gal. lat. (b)	-13.26°
Radial velocity	$5264 \pm 11\,\mathrm{km\,s^{-1}}$
Distance from cluster centre	0.0 Mpc
Luminosity distance	75.4 Mpc
Core flux density (5 GHz)	3.1 ± 0.16 Jy
Core power (5 GHz)	$2.1 \times 10^{24}\,\mathrm{W\,Hz^{-1}}$
Largest angular size	200 arcsec
Largest physical size	70 kpc
Total flux density (5 GHz)	23.3 Jy
Total power (5 GHz)	$1.6 \times 10^{25}\,\mathrm{W\,Hz^{-1}}$

We formed linear polarization images at constant resolution (see Fig. 2) for the purpose of comparing the polarization properties of 3C 84 as a function of frequency. The resolution in Fig. 2 is set by the 5-GHz observations and the higher frequencies have been tapered to provide matching resolution. Linear polarization is detected on November 11 from the bright jet component S1 in 3C 84 at 5, 8, 15 and 22 GHz at a level of 0.8–7.5 per cent increasing with frequency. Furthermore, there is some suggestion at 8.4 GHz and above that the polarization is extended. Similar results were obtained on October 26, but the leakage calibration was not as good at this epoch, so for the remainder of the discussion we focus on the November 11 results.

The detection of core polarization is less than 0.1 per cent for all frequencies except for 22 GHz for which it is 0.2 per cent. At this level the 14 mJy of linearly polarized flux density could well be significant. There is also some suggestion of polarization at 22 GHz in between the core and the end of the bright inner emission (component S1).

In Fig. 3, we present the RM image, a pixel-by-pixel fit to the polarization angle as a function of the square of the wavelength (λ^2). Since the 5-GHz observations were only weakly polarized and did not resolve S1, we have not included them in the fit. The eight frequencies included in the fit were 8.114, 8.184, 8.421, 8.594, 14.906, 14.972, 15.269, 15.368 and 22.233 GHz. The 15- and 22-GHz observations were tapered to match the 8.4-GHz resolution of $1.8 \times 1.3\,\mathrm{mas}^2$. Pixels were blanked if the statistical error in polarization angle exceeded 5° at any frequency. A representative fit at the peak of the polarized flux density of S1 is shown in Fig. 4. The systematic uncertainties in the polarization angle measurements were assumed to be $\sim 3^{\circ}$.

The RM corrected plot of the projected magnetic field orientation of the linearly polarized flux at 15 GHz is shown in Fig 5. The intrinsic magnetic field in the southern jet component S1 appears to be predominantly perpendicular to the jet axis, as expected if the field is enhanced by compression. The polarization angle of the core is uncertain given that the RM of the core is not well determined and is likely to be well in excess of $10\,000\,\mathrm{rad\,m^{-2}}$.

The RM image (Fig. 3) shows a gradient of about $1000\,\mathrm{rad\,m^{-2}\,pc^{-1}}$ across component S1 in the southern jet component. The statistical error in the RM determinations are $\sim 60\,\mathrm{rad\,m^{-2}}$, so it is likely that this gradient is real. It is possible that spectral effects (see Fig. 6) and substructure at the high frequencies cause some departures from a λ^2 law. There is significant depolarization (9.5 per cent at 15.3 GHz to 3.5 per cent at 8.2 GHz at $\sim$1.5-mas resolution) in the southern hotspot. This depolarization, and that seen between 5 and 22 GHz in a larger beam, are consistent with beamwidth depolarization by the observed RM gradient.

It is worth noting that the RM decreases with increasing distance from the centre of the lobe, i.e. the gradient slopes down in the direction of the edge of the lobe. This indicates that the density and/or the field strength decreases towards the edge. This situation is reminiscent of that in M87 where no polarization is detected in the bright inner few pc (Zavala & Taylor 2002), and is most naturally explained by a radial falloff in the density. Polarization is not expected from the counterjet in 3C 84, both because it is fainter, and because it is behind a denser Faraday screen.

We note that Homan & Wardle (2004) found strong circular polarization in the central pc of 3C 84, reaching +3 per cent at 15 GHz. They speculate that the circular polarization may be produced by Faraday conversion of linear to circular polarization. No circular polarization was detected by Homan & Wardle (2004) from the bright southern jet at 15 or 22 GHz, and the linear polarization from the central pc was found to be less than 1 per cent.

5 DISCUSSION

5.1 Magnetic fields in Perseus

For a refractive medium in the presence of magnetic fields the intrinsic polarization angle, χ_0, is observed as χ such that

$$\chi = \chi_0 + \mathrm{RM}\lambda^2, \tag{1}$$

where λ is the observed wavelength. The RM is related to the electron density, n_e, the net line of sight magnetic field in the environment, $B_\parallel$, and the path length, dl, through the plasma, by the equation

$$\mathrm{RM} = 812 \int n_e B_\parallel \,\mathrm{d}l\ \mathrm{rad\,m^{-2}}, \tag{2}$$

where units are in $\mathrm{cm^{-3}}$, μG and kpc. Our best estimate from Section 3 for n_e is $0.3\,\mathrm{cm^{-3}}$. We assume a path length of 2 kpc, which probes the highest density gas in the cluster, and is typical of RM scale sizes in other cooling core clusters (Carilli & Taylor 2002). Assuming a constant magnetic field orientation, we find a magnetic field strength of 15 μG. This is only the component along the line-of-sight, so correcting by a factor of $\sqrt{3}$, we estimate a field strength of 25 μG.

Field strengths calculated with these parameters can be compared to the strength of a magnetic field that has the same pressure as a gas of the same n_e and a temperature of 5×10^7 K using

$$\frac{B^2}{8\pi} = 2 n_e k T. \tag{3}$$

In the central ($r < 2$ kpc) region of the Perseus cluster we find this gives 300 μG, so the magnetic pressure from the estimated field strength of 25 μG is two orders of magnitude less than the thermal pressure ($\sim 4 \times 10^{-9}\,\mathrm{dyn\,cm^{-2}}$). This result is similar to that found in other cooling core clusters.

A difficulty with producing the RMs in 3C 84 in the ICM is that the observed gradient of 10 per cent of the RM on scales of $\sim$1 pc is hard to reconcile with fields organized on kpc scales.

5.2 The high-velocity system

Emission- and absorption-line studies have highlighted the existence of a high-velocity system (at $\sim 8200\,\mathrm{km\,s^{-1}}$) at approximately

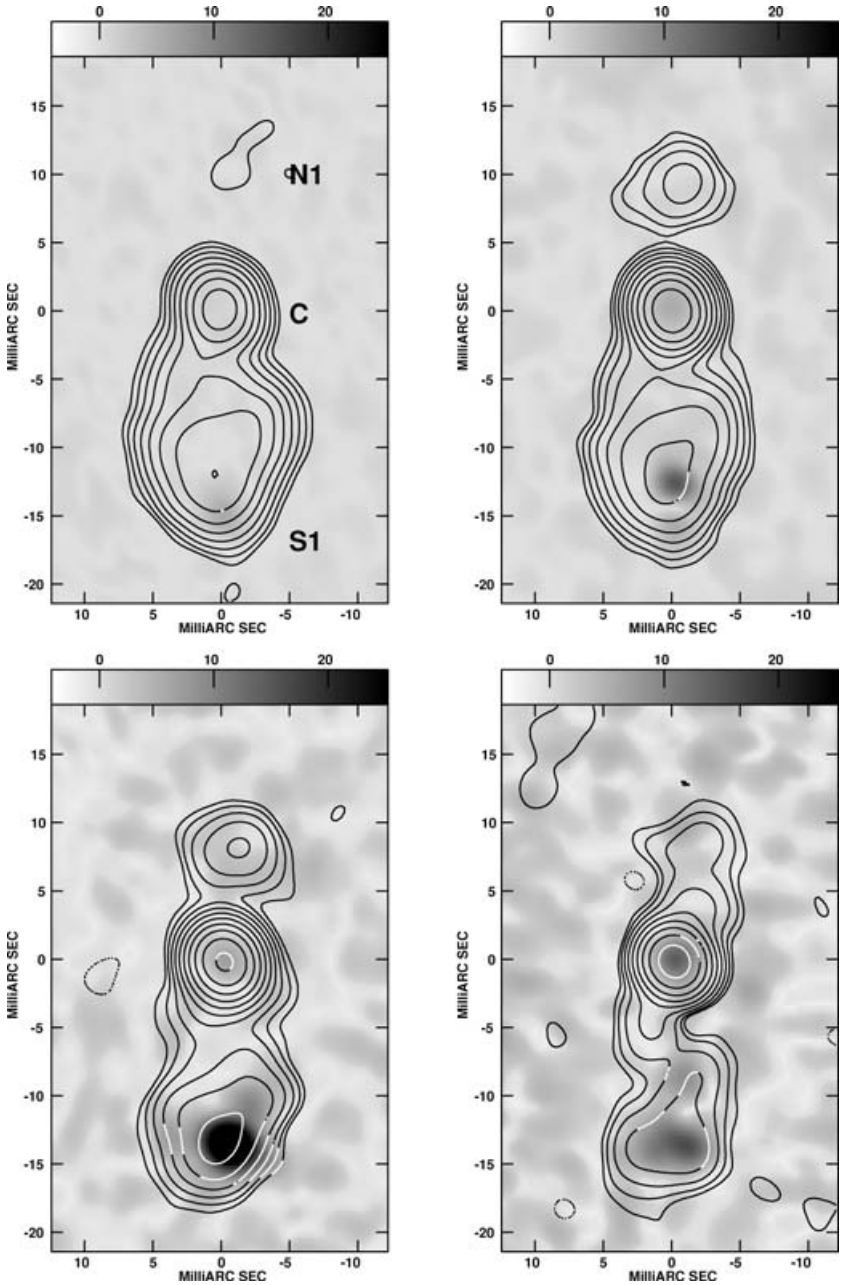

Figure 2. VLBA observations of 3C 84 at 5, 8, 15 and 22 GHz at a fixed angular resolution of 2.75 mas. The grey-scale represents linearly polarized intensity ranging from -4 to 2 mJy beam^{-1} in all panels. Contour levels begin at 15 mJy beam^{-1} and increase by a factor of 2. Coordinates are relative to the VLBA pointing centre at J2000 RA $03^{\rm h}19^{\rm m}48\overset{\rm s}{.}16$, Dec. $41^\circ30'42\overset{''}{.}1$.

the same position on the sky as NGC 1275 (which has a systemic velocity of $\sim$5200 km s^{-1}). This system is likely to be associated with a spiral galaxy falling into the Perseus cluster at 3000 km s^{-1}. Recently Gillmon, Sanders & Fabian (2004) have shown through the study of the X-ray absorption that this system is not interacting with the body of NGC 1275 and that they are separated by at least 57 kpc.

Can this spiral galaxy be responsible for the observed RMs? The hot component of its interstellar medium (ISM) is not likely to produce the observed RMs, as the required density (assuming a $B_\parallel$ of 3 μG, a path length of 10 kpc and a temperature of 10^5 K) is 0.3 cm^{-3}, about two orders of magnitudes larger than one would infer from a simple pressure equilibrium argument with the neutral component of the ISM, whose density and temperature were estimated by Momjian, Romney & Troland (2002). The possibility that a very compact H II region belonging to the high-velocity system might be responsible for the observed RMs cannot be completely excluded, even though the probability of finding such a region directly along our line-of-sight to the core of NGC 1275 is very small.

5.3 The ionized filaments

The filamentary structure of ionized gas associated with NGC 1275, instead, might well produce the observed RMs: the Hα observations

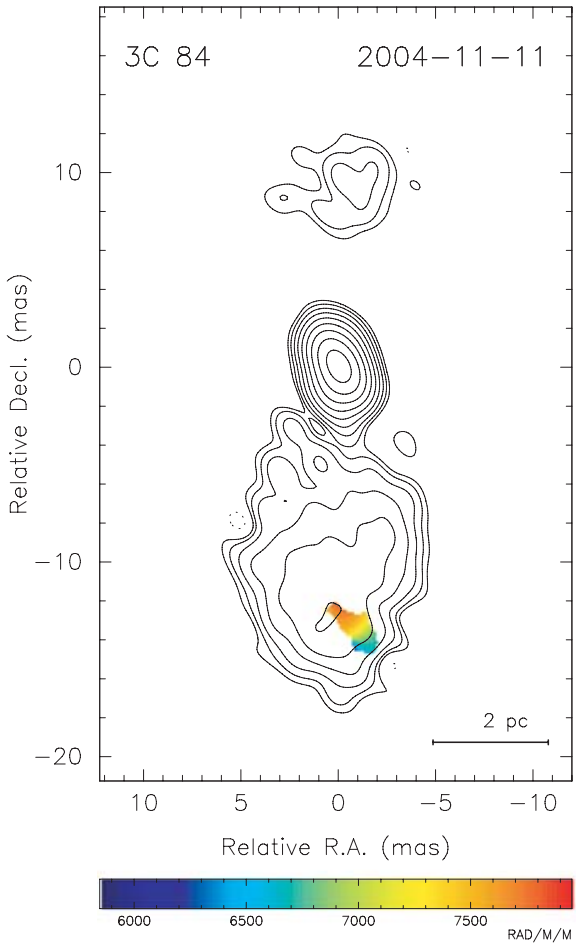

Figure 3. RM image of 3C 84 at 1.8 × 1.3 mas^2 resolution in position angle 30°. Contour levels from the 8 GHz total intensity image begin at 15 mJy beam^{-1} and increase by a factor of 2.

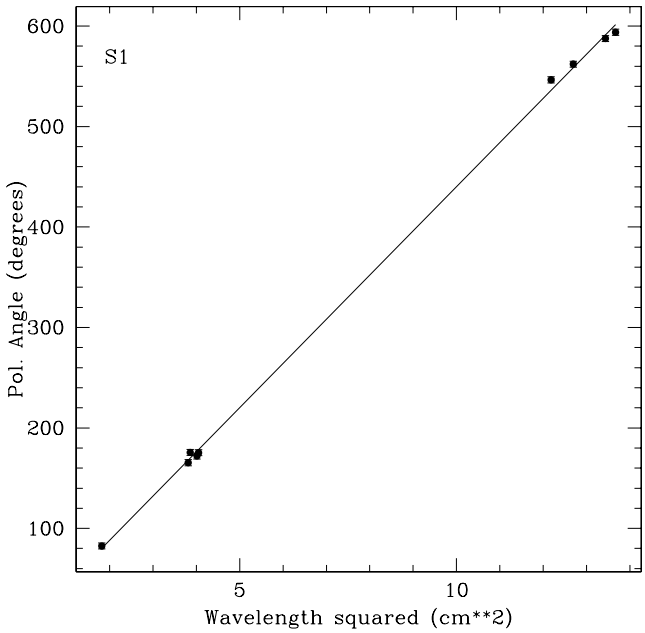

Figure 4. Position angle versus λ^2 for the southern component. The fit gives the Faraday RM of 7680 ± 64 rad m^{-2}.

performed by Conselice, Gallagher & Wyse (2001) showed the presence of unresolved features with size less than ∼230 pc and lower bound electron densities of $\geqslant$10 cm^{-3}. Densities measured in the [S II] lines in the central kpc are 270 cm^{-3} (Johnstone & Fabian 1988; Heckman et al. 1989), and the optical filaments are thought to be in equipartition with the ICM with pressures of $\sim 1 \times 10^{-9}$ dyn cm^{-2}. Comparing the central surface brightness in Hβ with emission from gas at the X-ray pressure (Fabian et al. 2003) near the centre of the cluster gives a depth of 0.06 pc for a temperature of 10^4 K and a uniform covering fraction, f. If the filaments are more filamentary than sheet-like, then the depth of the Hβ increases in proportion to $1/f$, but it becomes difficult with a small covering factor to produce coherent RMs across the radio source. Also, if the surface brightness of the Hβ line rises close to the nucleus where it is unresolved, then this can increase the estimate of the depth. Observations in the Paα line (Wilman, Edge & Johnstone 2005) indicate that the surface brightness does rise by one to two orders of magnitude within the inner 150 pc. This increases the above estimate for the depth of the filaments from the Hβ line to at least 1 pc.

The small size of the ionized filaments could explain the 10 per cent gradient in the RM on scales of a pc. Assuming a constant gradient we might use this to estimate a scale size for the RMs of ∼10 pc. Assuming that the scale size along the line-of-sight is similar to that in the plane of the sky leads to an estimate for the Faraday depth of ∼10 pc.

With the above density and path length (10 pc) and the observed RM, we obtain a lower limit for $B_\parallel$ of 4 μG, and hence a magnetic pressure of $\sim 2 \times 10^{-12}$ dyn cm^{-2}, nearly three orders of magnitude below the thermal pressure. If the filaments are as small as 1 pc (with a uniform covering factor, $f = 1$), then the field strength required to produce the observed RMs is $B \sim 50$ μG, but the magnetic pressure is still less than the thermal pressure by a factor of ∼4.

It is also possible that the radio source is interacting with the ionized gas and that the densities are enhanced at the southern edge of the expanding source, which appears reminiscent of a bow-shock. Locally higher densities would further reduce the strength of the magnetic fields required to produce the observed RMs. Similar magnitude RMs have been detected in a few other well studied radio galaxies (e.g. M87, 3C 120; Zavala & Taylor 2002), and attributed to ionized gas in close proximity to the radio emission. Baum et al. (2005) have shown that there is no significant column density of more neutral gas along the line of sight to the nucleus from the lack of any strong Lyα absorption.

We note that the observed decrease in fractional polarization with wavelength can be attributed to gradients in the Faraday screen.

6 CONCLUSIONS

We find substantial Faraday RMs of ∼7000 rad m^{-2} toward 3C 84. RMs as large or larger than this have been suspected for some time due to the low observed polarization from this bright radio galaxy. The Faraday screen is most likely to be associated with the ionized gas that also produces spectacular filaments of Hα emission in the Perseus cluster. This gas may well have magnetic fields organized on small enough scales (<10 pc), to produce the observed gradient in the RM.

Our current measurements provide only a few very closely spaced lines-of-sight through the cluster. To establish the scale size over which the magnetic fields are organized, and to look for

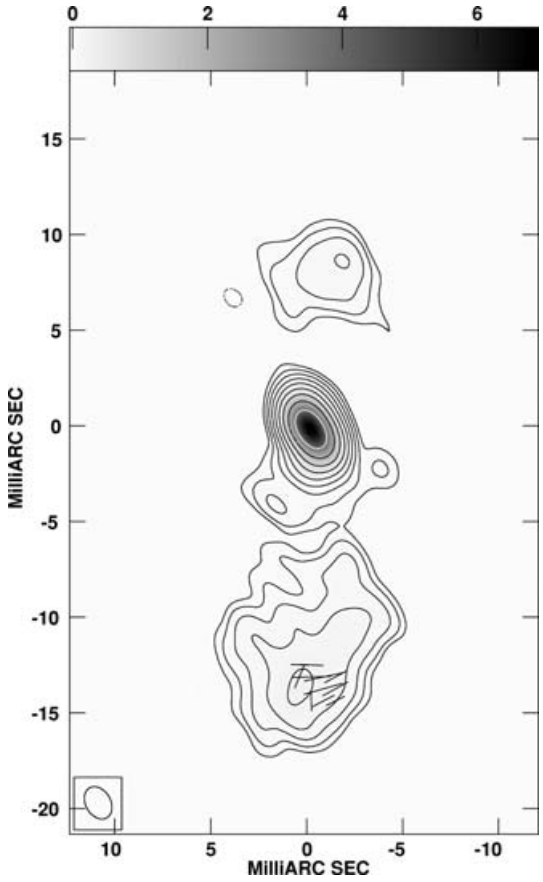

Figure 5. The RM corrected magnetic field (B) vectors at 15 GHz overlaid on a total intensity image at $1.8 \times 1.3\,\mathrm{mas}^2$ resolution in position angle 30°. The length of the vectors is proportional to polarized flux density. Contour levels begin at $15\,\mathrm{mJy\,beam}^{-1}$ and increase by a factor of 2.

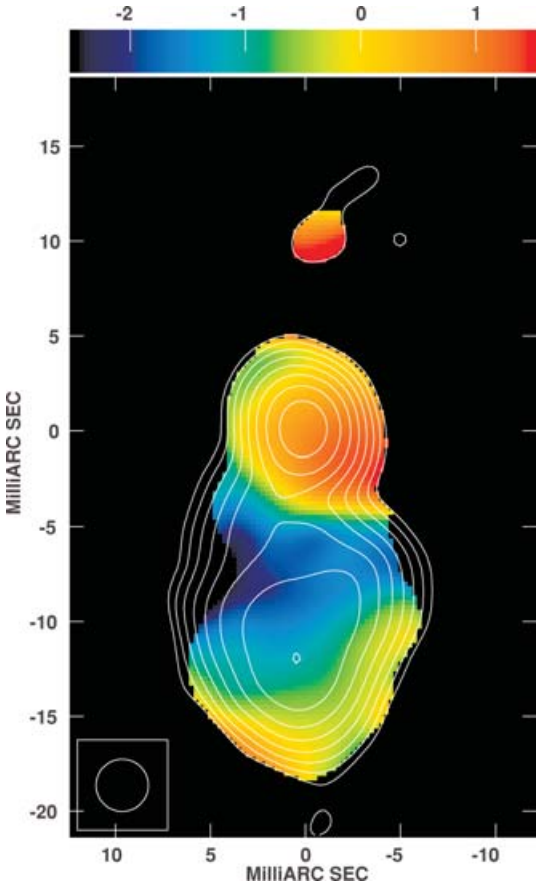

Figure 6. The spectral index image, defined $S_\nu \propto \nu^\alpha$, between 5 and 15 GHz overlaid on the 5 GHz total intensity image at 2.75-mas resolution. Contour levels begin at $15\,\mathrm{mJy\,beam}^{-1}$ and increase by a factor of 2.

correlations with the cavities seen in the X-ray emission, we would like to be able to sample the RM distribution in the Perseus cluster on scales out to many 10s kpc. There is fairly strong radio emission on these scales, but detecting the polarization is challenging. To determine RMs in larger regions, we have to have greater sensitivity to extended emission than the VLBA provides. But increasing the beam size means more susceptibility to RM gradients within the beam. It also means that the flux within the central resolution element goes up (quite dramatically when components C and S1 merge) so the required dynamic range increases as well. Errors in the leakage calibration are typically ∼0.5 per cent for individual antennas and will average out over an array by $\sim N^{1/2}$, where N is the number of elements in the array; errors are further reduced away from the image centre by an additional factor of $N^{1/2}$ (Roberts, Wardle & Brown 1994). These errors scale with the total intensity so that a point source of 10 Jy produces a linear polarization noise floor of $\sim 5\,\mathrm{mJy\,beam}^{-1}$ for the VLBA and $\sim 2\,\mathrm{mJy\,beam}^{-1}$ for the VLA.

An array like the proposed EVLA phase 2 with 35 antennas, excellent sensitivity, and subarcsecond resolution could have a good chance of detecting polarization from a larger region across 3C 84 at high frequencies. The EVLA phase 1 currently under construction has less resolution than desired, but if the errors in the leakage terms can be reduced below 0.5 per cent, then it might be possible for some regions where the gradient happens to be low to be measured. This will also become easier in time so long as 3C 84 continues to fade at centimetre wavelengths (Aller, Aller & Hughes 2003).

Future VLBA observations of 3C 84 to look for changes in the RM distribution with time could provide additional information about the nature of the Faraday screen.

ACKNOWLEDGMENTS

We are grateful to the referee, Daniel Homan, for insightful suggestions. GBT acknowledges support for this work from the National Aeronautics and Space Administration through *Chandra* Award Number GO4-5134A issued by the *Chandra* X-ray Observatory Centre, which is operated by the Smithsonian Astrophysical Observatory for and on behalf of the National Aeronautics and Space Administration under contract NAS8-03060. NEG gratefully acknowledges support from the NRAO Graduate Summer Student Research Assistantship. This research has made use of the NASA/IPAC Extragalactic Database (NED) which is operated by the Jet Propulsion Laboratory, Caltech, under contract with NASA. The National Radio Astronomy Observatory is a facility of the National Science Foundation operated under a cooperative agreement by Associated Universities, Inc.

REFERENCES

Aller M. F., Aller H. D., Hughes P. A., 2003, ApJ, 586, 33
Baum S. A., Laor A., O'Dea C. P., Mack J., Koekemoer A. M., 2005, ApJ, 632, 122

Burns J. O., 1990, AJ, 99, 14
Carilli C. L., Taylor G. B., 2002, ARA&A, 40, 319
Conselice C. J., Gallagher J. S., III, Wyse R. F. G., 2001, AJ, 122, 2281
Fabian A. C., Sanders J. S., Crawford C. S., Conselice C. J., Gallagher J. S., Wyse R. F. G., 2003, MNRAS, 344, L48
Fabian A. C., Sanders J. S., Taylor G. B., Allen S. W., 2005a, MNRAS, 360, L20
Fabian A. C., Reynolds C. S., Taylor G. B., Dunn R. J. H., 2005b, MNRAS, 363, 891
Fabian A. C., Sanders J. S., Taylor G. B., Allen S. W., Crawford C. S., Johnstone R. M., Iwasawa K., 2006, MNRAS, 366, 417
Feretti L., Dallacasa D., Govoni F., Giovannini G., Taylor G. B., Klein U., 1999, A&A, 344, 472
Gillmon K., Sanders J. S., Fabian A. C., 2004, MNRAS, 348, 159
Gugliucci N. E., Taylor G. B., Peck A. B., Giroletti M., 2005, ApJ, submitted
Heckman T. M., Baum S. A., van Breugel W. J. M., McCarthy P., 1989, ApJ, 338, 48
Homan D. C., Wardle J. F. C., 2004, ApJ, 602, L13
Huchra J. P., Vogeley M. S., Geller M. J., 1999, ApJS, 121, 287
Johnstone R. M., Fabian A. C., 1988, MNRAS, 233, 581
Kellermann K. I., Pauliny-Toth I. I. K., 1968, ARA&A, 6, 417
Momjian E., Romney J. D., Troland T. H., 2002, ApJ, 566, 195
Roberts D. H., Wardle J. F. C., Brown L. F., 1994, ApJ, 427, 718
Silver C. S., Taylor G. B., Vermeulen R. C., 1998, ApJ, 502, 229
Taylor G. B., Myers S. T., 2000, VLBA Scientific Memo 26. National Radio Astronomy Observatory, Charlottesville, VA
Taylor G. B., Vermeulen R. C., 1996, ApJ, 457, L69
Taylor G. B., Barton E. J., Ge J., 1994, AJ, 107, 1942
Vermeulen R. C., Readhead A. C. S., Backer D. C., 1994, ApJ, 430, L41
Vogt C., Enßlin T. A., 2005, A&A, 434, 67
Walker R. C., Dhawan V., Romney J. D., Kellermann K. I., Vermeulen R. C., 2000, ApJ, 530, 233
Wilman R. J., Edge A. C., Johnstone R. M., 2005, MNRAS, 359, 755
Zavala R. T., Taylor G. B., 2002, ApJ, 566, L9

This paper has been typeset from a TEX/LATEX file prepared by the author.